

## **Seismic Response Analysis of the Foundation Area of the Acheloos River Dam (Central Greece) as Determined from a Seismic Refraction Survey and the Boundary-Element Method**

G.-A. TSELENTIS, C. THANASSOULAS and G. STAVRAKAKIS

*University of Athens, Dept. of Geophysics and Geothermy, Panepistimiopolis, Athens 15701 (Greece)*

*Institute of Geology and Mineral Exploration, Geophysics Div., 57 Mesoghion Ave., Athens (Greece)*

*Earthquake Planning and Protection Organization, 196-198 Ippocratous Str., Athens 114-71 (Greece)*

(Received January 8, 1986; accepted after revision July 7, 1986)

### ABSTRACT

Tselentis, G.-A., Thanassoulas, C. and Stavrakakis, G., 1987. Seismic response analysis of the foundation area of the Acheloos river dam (Central Greece) as determined from a seismic refraction survey and the boundary-element method. *Geoexploration*, 24: 197-206.

An extensive seismic refraction survey in the foundation area of the Acheloos river dam (Central Greece), revealed the existence of four layers.

The P and S seismic wave velocities of these layers were measured and used in a two-dimensional boundary-element model of the area to determine its dynamic behaviour when subjected to incident SH waves from strong earthquakes.

The results of the analysis showed that the frequency response curves for incident angles of 0° and 45° depend upon the thickness of the sediments and that there is a considerable difference in the response characteristics from site to site towards the higher frequencies.

Also, the calculation of the maximum amplification factor showed that it increases towards the centre of the valley.

### INTRODUCTION

It is well known that the ground motion experienced at a given observation point following an earthquake may be significantly affected by the near-surface geological configuration at the specific site.

Since geological and topographic irregularities in the soil medium seem to have a tremendous effect on the characteristics of the ground motion due to

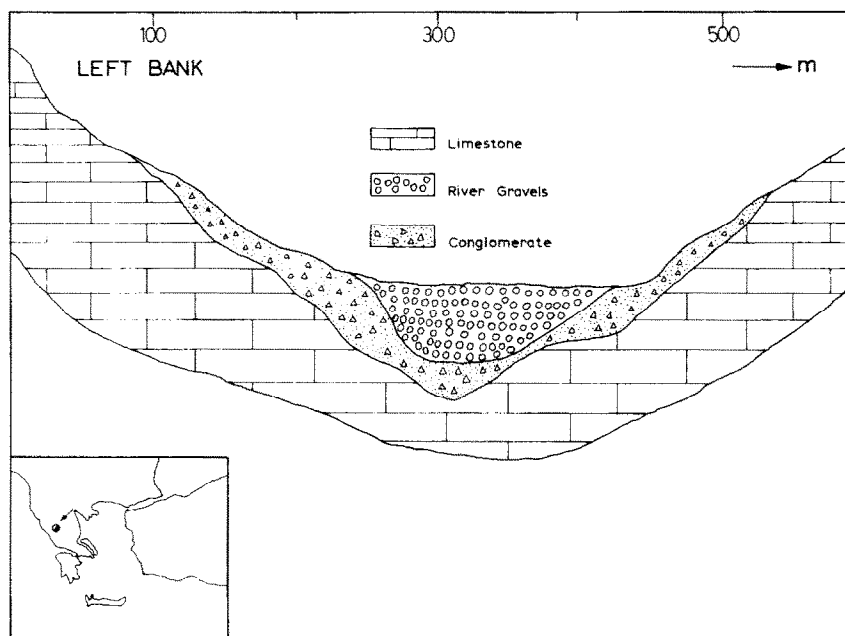


Fig. 1. Typical geological section across the valley.

an earthquake, in attempting to predict ground-motion characteristics one must deal with the problem of estimating the magnitude of the effect of the recording-site geology in terms of observable physical parameters such as those usually obtained from geophysical investigations.

The present investigation was made to determine the dynamic behaviour of the foundation area of the Acheloos river dam (Central Greece), and consists of two parts: (1) a detailed mapping of the structure of the deep layer in the area using seismic refraction methods; (2) the solution of the elastodynamic field equation for incident SH-waves, using the boundary-element method.

#### GEOLOGICAL SETTING OF THE AREA

The area under investigation is a part of the valley of the river Pamissos which is an affluent of the Acheloos river. The basement of the valley is covered by a thick layer of riverbed alluvium consisting of two parts: (a) a thick layer of river gravels which covers the axes of the valley and in some areas reaches a thickness of 40–50 m; (b) a coarse sandy gravel (conglomerate) in a fairly dense state.

A typical geological section of the valley as deduced from the geoseismic profiles and the borehole is shown in Fig. 1.

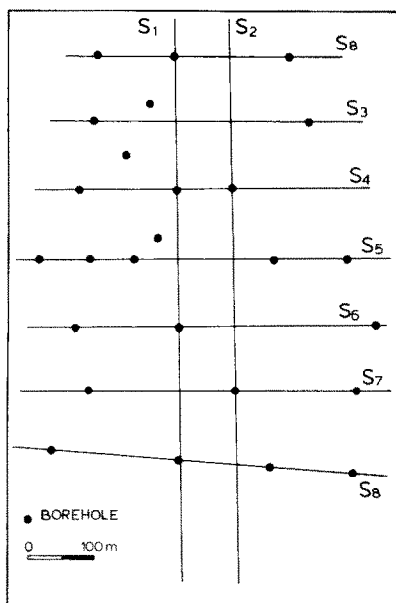


Fig. 2. Seismic traverses and boreholes.

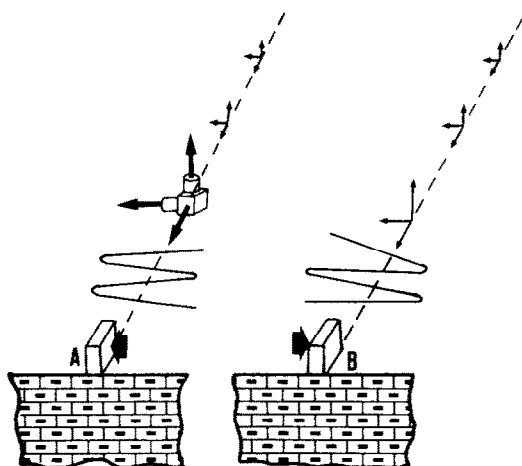


Fig. 3. Geophone arrangement used for SH-wave measurements.

### SEISMIC REFRACTION INVESTIGATIONS

The area of interest was covered by 5.4 km of seismic refraction lines (traverses); two of these were shot parallel to the axis of the valley and the rest perpendicular to it (Fig. 2).

Each traverse consisted of a number of 12-geophone spreads with 10 m intervals between geophones and two geophones overlapping.

The source used was explosive charges placed in shotholes 1 m deep. In each spread, seven shots were fired and the cumulative travel-time graph was formed by adding the differences in arrival times at overlapping pairs of geophones cumulatively to the arrival times at geophones further along the line.

To obtain a depth profile of the layers encountered in the area from the seismic data, the plus-minus method (Sjogren, 1984) was used.

In addition to the above techniques, in certain parts of the area, where unweathered outcrops of the main geologic formations could be located, special S-wave measurements were carried out using a 6.3 kg shear-wave hammer source.

The basic equipment used for the recording of the arrivals was an ABEM TRIO SX-12 twelve-channel portable seismic refraction recorder/amplifier system.

The geophones were attached to small metallic blocks which were cemented

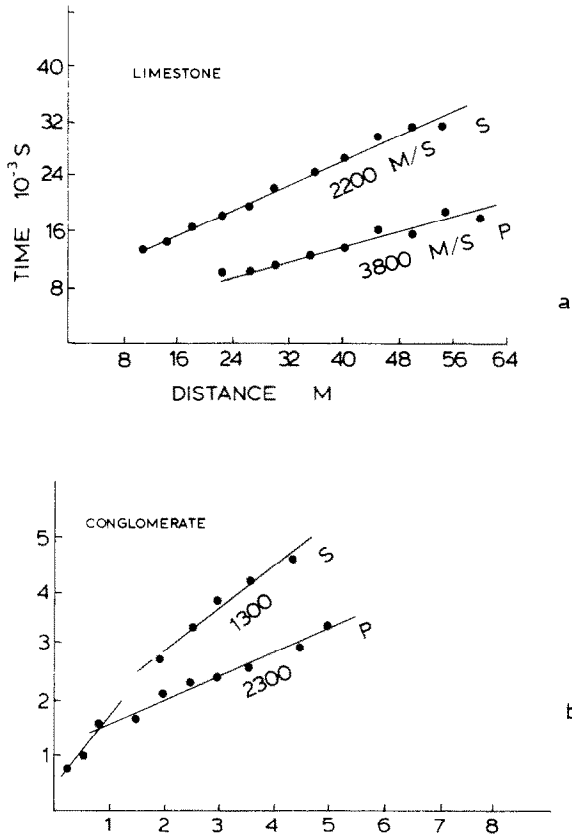


Fig. 4. Travel-time curves showing  $V_p$  and  $V_s$  values for the limestone and the conglomerate.

in place in the ground with chemical cement. We used two geophones per block, one in the vertical direction and one horizontally orientated at  $90^\circ$  to the profile line.

A hammer with a mercury switch to start the TRIO recorder and an impact switch for generating the time-break signal was used. We used two impacts at either side of the ground pole (left-right), so that we observed a  $180^\circ$  polarity reversal in the seismograms obtained. This helped in picking the correct arrival times for the S-waves (Fig. 3).

Two travel-time curves, with the  $V_p$  and  $V_s$  for the limestone and the conglomerate formations, are shown in Fig. 4. Although the velocities obtained correspond to the upper part of the formations and may change at great depths, we made the assumption that these are representative values for all the formations considered. On the other hand, seismic velocities which were determined for a number of cores in the laboratory (using an OYO Sonicviewer) did not show considerable variation with depth.

## BOUNDARY-ELEMENT FORMULATION

Boundary integral techniques are becoming increasingly popular in geophysics as well as in other engineering fields.

The use of boundary integral equations to solve seismic-wave propagation problems numerically is a fairly recent development (Shippy, 1975; Shaw, 1979). The analogy between the interpolation functions in the integral-equation approach and those in the finite-element method has been noticed and the term "boundary-element method" is frequently used (Brebbia, 1978).

In essence, the boundary-element method works with the fundamental solutions as influence functions and it tries to satisfy the boundary conditions at the inhomogeneous interfaces.

In the present work, the elastodynamic field equation is reduced to a two-dimensional Helmholtz equation for SH-wave incidence:

$$\frac{\partial^2 u_j}{\partial x^2} + \frac{\partial^2 u_j}{\partial y^2} + k_j^2 u_j = 0 \quad (1)$$

where  $k_j = \omega/b_j$  is the wave number, in which  $\omega$  is the circular frequency,  $b_j$  is the shear-wave velocity in soil medium  $j$ .

It can be shown (Brebbia, 1978), that the fundamental solution of eq. 1 is given by:

$$u_j = iH_0^2(k_j r)/4 \quad (2)$$

where  $H_0^2$  is a Hankel function of zero order of second kind and  $r$  is the distance between the observation and source points.

The boundary-element network of the layer model of the area which was used in the following analysis is shown in Fig. 5a.

Using the fundamental solution as a particular type of weighting function, the boundary-element formulation of eq. 1 can be written as follows:

$$c_j u_j + \sum_1^N \int u t dB = \sum_1^N \int t u dB \quad (3)$$

where  $t$  is the traction (stress) on the boundary  $B$ , and the value of  $c_j$  depends on the type of boundary being considered. The nodes are considered to be at the intersection between two straight elements, and the variation in the unknown  $t$ 's and  $u$ 's is assumed to be linear within each element (Fig. 5a).

Obviously, eq. 3 relates the value of  $u$  at point  $j$  to the values of  $t$  and  $u$  over the boundary, and can be written in the following matrix form (see Appendix I):

$$\sum_1^N H_{ji} u_i = \sum_1^N G_{ji} t_i \quad (4)$$

or as follows:

$$t = ku, \quad k = g^{-1}h \quad (5)$$

where  $t$  and  $u$  are the traction and displacement vectors of order  $n$ ,  $k$  is the stiffness matrix (Davis, 1980) that gives the relationship between stress and displacement at nodal points in a certain element  $n$ , and  $g$  and  $h$  are defined in Appendix I.

## NUMERICAL SOLUTION

To analyze the seismic response of the foundation site to incident SH-waves, the model derived from the seismic refraction investigations was subdivided into a fairly large number of nodal points ( $N=46$ ), as shown in Fig. 5.

For each element, the stiffness matrix  $k_n$  ( $n=1, 2, \dots, N$ ) can be calculated using eq. 5. The zone is divided into zone I and an infinite half space II.

The equation of motion for zone I is given in matrix form by superposing the stiffness matrix of each element in region I and bearing in mind the scattered wave field:

$$\begin{bmatrix} K_{BB} & K_{BI} \\ K_{IB} & K_{II} \end{bmatrix} \cdot \begin{bmatrix} U_B \\ U_I \end{bmatrix} = \begin{bmatrix} T_B \\ T_I \end{bmatrix} \quad (6)$$

where the subscripts I and II are added to variables in domains I and II, respectively, and  $U_B$  and  $T_B$  are the deformation and traction values of nodal points of the boundary B.

The equation of motion for the scattering wave is given by the following matrix form:

$$K_C U_C = T_C \quad (7)$$

where  $K_C$  is the stiffness matrix and  $U_C$  and  $T_C$  are the nodal displacement and traction on the boundary B which are derived from the scattering wave field (Fig. 5c).

Eq. 7, when combined with the following boundary conditions on B:

$$U_B = U_C + U_0, \quad T_B + T_C + T_0 = 0 \quad (8)$$

yields:

$$T_B = -K_C U_B - T_0 + K_C U_0 \quad (9)$$

where  $U_0$  and  $T_0$  are the displacement and traction of the nodal points on the boundary due to incident waves that can be calculated from the solution in the homogeneous half space with the imaginary ground surface  $g_1-g_2$  (Fig. 5d) and the incident wave field  $w$  (Trifunac, 1971). Thus eq. 6 can be written as:

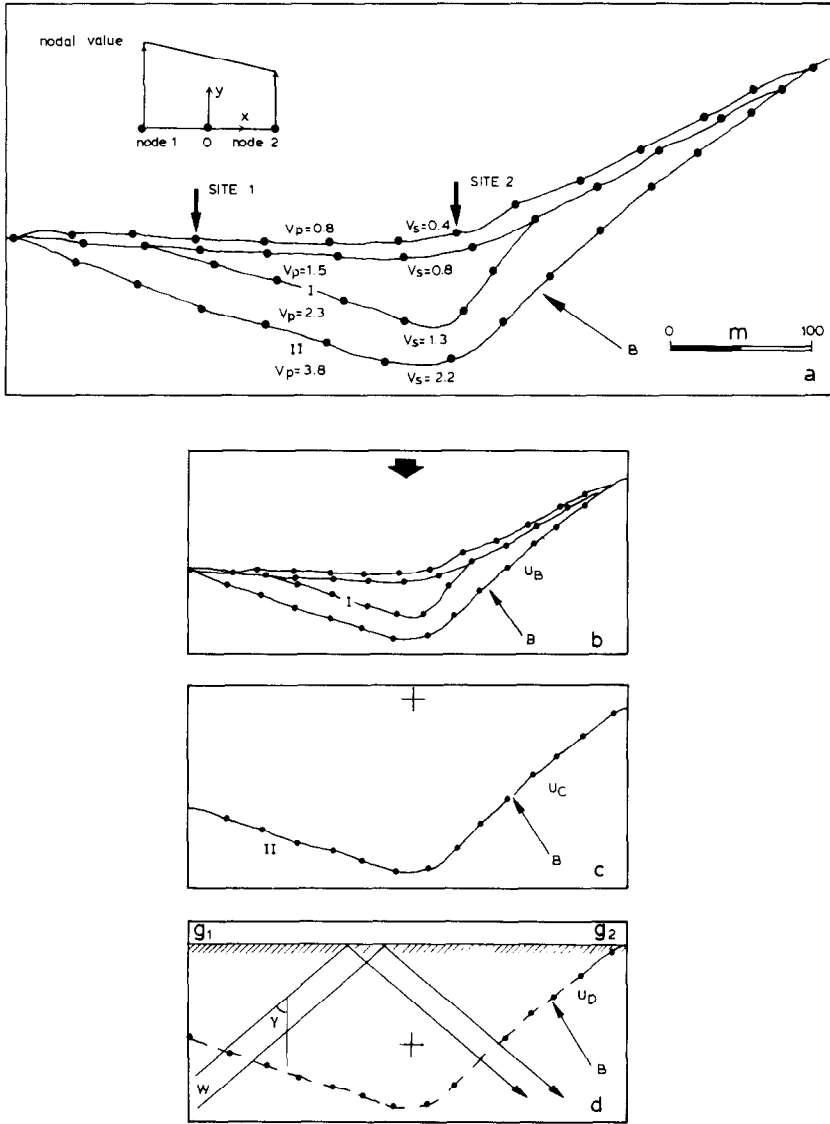


Fig. 5. Ground discretized by the boundary-element method.

$$\begin{bmatrix} K_{BB} + K_C & K_{BI} \\ K_{IB} & K_{II} \end{bmatrix} \cdot \begin{bmatrix} U_B \\ U_I \end{bmatrix} = \begin{bmatrix} K_C U_0 - T_0 \\ T_I \end{bmatrix} \quad (10)$$

SURFACE DISPLACEMENT SPECTRA

A question of primary interest is the spatial and frequency dependence of

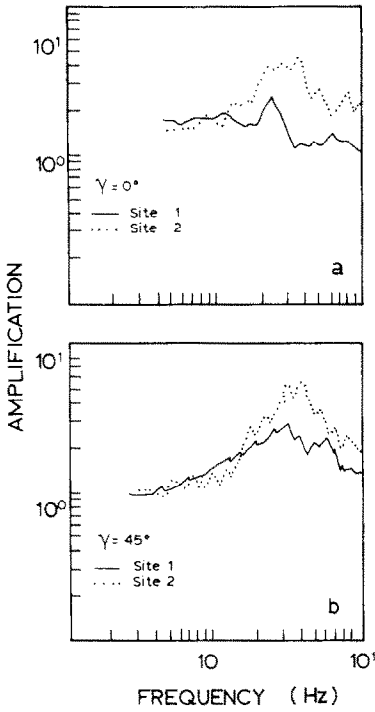


Fig. 6. Amplification factors at sites 1 and 2 (see Fig. 5a).

the ground motion due to a strong earthquake. For the case investigated in the present paper, we assume the excitation to be a steady train of propagating SH-waves of amplitude 1 and frequency  $\omega$ , travelling along a ray which makes an angle  $\gamma$  with the vertical. Obviously, these waves can be described by the following equation:

$$u_{\gamma}^i = e^{i\omega\{t - (x/c_x) + (y/c_y)\}} \quad (11)$$

where  $c_x = \beta/\sin\gamma$  and  $c_y = \beta/\cos\gamma$  are the phase velocities along the  $x$  and  $y$  axes, respectively, and  $\beta$  is the shear-wave velocity.

The solution given by eq. 5 obviously gives spectral amplitudes, since the amplitude of incident waves is taken to be unity.

Consider a mean unit weight of  $2.0 \text{ t/m}^3$  for the area and the respective wave velocities shown in Fig. 5a. The frequency-response curves for incident angles of  $0^\circ$  and  $45^\circ$  at two locations along the valley are shown in Fig. 6.

Judging from these figures, we see that there is a considerable difference in the response characteristics of the two sites which increases towards the higher frequencies.

The above process was repeated for all the points across the valley at 50 m intervals and Fig. 7 gives the maximum amplification factor obtained for an incident angle of  $0^\circ$ .



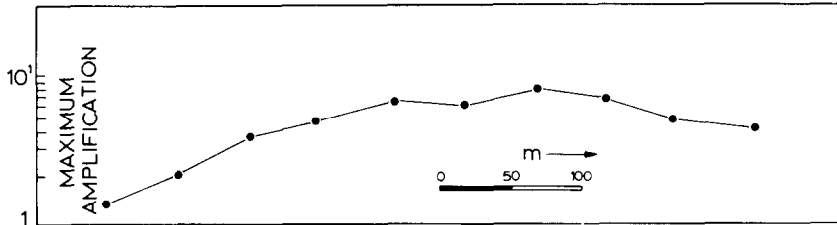


Fig. 7. Maximum amplification factor across the valley for frequencies up to 10 Hz.

## CONCLUSIONS

The method of boundary integral equations has been presented to examine the effect of local geological and topographic site conditions on the dynamic characteristics of the foundation area of the Acheloos river dam.

A detailed seismic refraction investigation incorporating P and S wave techniques was carried out to determine the deep layer structure of the area.

The results obtained showed that the boundary-element method, when combined with geophysical prospecting, can be a very powerful tool for analyzing the seismic response of building sites with a generally irregular soil profile beneath the ground surface.

## ACKNOWLEDGEMENTS

The authors wish to thank Mr. N. Kazilis, engineering geologist of the Public Electric Organization of Greece for his help during the field work and Dr. A. Sofianos of the Rock Mechanics Dept. of Imperial College of Science and Technology of the University of London for his help with programming the computer code.

## APPENDIX I - PROOF OF EQ. 4

Consider the linear element shown in Fig. 3a. The values of  $u$  and  $t$  at any point of the element are defined in terms of their nodal values and the linear interpolation functions  $\phi_1$  and  $\phi_2$ . Thus, we can write:

$$u(\xi) = [\phi_1 \phi_2] \begin{bmatrix} u_1 \\ u_2 \end{bmatrix} \quad t(\xi) = [\phi_1 \phi_2] \begin{bmatrix} t_1 \\ t_2 \end{bmatrix} \quad (\text{A1})$$

where the dimensionless coordinate  $\xi = 2x/1$  and  $\phi_1$  and  $\phi_2$  are given by:

$$\phi_1 = (1 - \xi)/2 \quad \text{and} \quad \phi_2 = (1 + \xi)/2 \quad (\text{A2})$$

The integrals along an  $i$  element in eq. 3 become:

$$\int utdB = \int [\phi_1 \phi_2] t dB \quad \begin{bmatrix} u_1 \\ u_2 \end{bmatrix} = (h_{i1} h_{i2}) \quad \begin{bmatrix} u_1 \\ u_2 \end{bmatrix} \quad (\text{A3})$$

where:

$$h_{i1} = \int \phi_1 t dB, h_{i2} = \int \phi_2 t dB$$

Similarly:

$$\int tudB = [g_{i1} g_{i2}] \quad \begin{bmatrix} t_1 \\ t_2 \end{bmatrix}$$

where:

$$g_{i1} = \int \phi_1 u dB \quad \text{and} \quad g_{i2} = \int \phi_2 u dB$$

In the present work, the integrals were calculated using a 4-point Gaussian quadrature rule for all segments.

Thus, eq. 3 can be written for the  $j$  element in the following assembled form:

$$C_j u_j + (\hat{H}_{j1}, \dots, \hat{H}_{jn}) \begin{bmatrix} u_1 \\ u_2 \\ \cdot \\ \cdot \\ u_n \end{bmatrix} = (G_{j1}, \dots, G_{jn}) \begin{bmatrix} t_1 \\ t_2 \\ \cdot \\ \cdot \\ t_n \end{bmatrix} \quad (\text{A4})$$

where  $\hat{H}_{j1} = h_{j1} + h_{j2}$  for element  $i$  and similarly for  $G_{ji}$ .

Obviously, eq. A4 can be written as:

$$\sum_1^N H_{ji} u_i = \sum_1^N G_{ji} t_i \quad (\text{A5})$$

with  $H_{ji} = \hat{H}_{ji}$  when  $j = i$ ,  $H_{ji} = \hat{H}_{ji} + C_j$  when  $j \neq i$ .

## REFERENCES

- Brebbia, C.A., 1978. *The Boundary Element Method for Engineers*. Pentech Press, London, 189 pp.
- Davis, A.J., 1980. *The Finite Element Method*. Clarendon Press, Oxford, 287 pp.
- Shaw, R.P., 1979. Boundary integral equation methods applied to wave problems. In: P. Banerjee and R. Butterfield (Editors), *Developments in Boundary Element Methods*. Applied Science Publishers Ltd., London, pp. 121-154.
- Shippy, D.J., 1975. Application of the boundary integral equation method to transient phenomena in solids. In: T. Cruse and F. Rizzo (Editors), *Boundary Integral Equation Method: Computational Applications in Applied Mechanics*. AMD, Vol. 11, ASME, New York, N.Y.
- Sjogren, B., 1984. *Shallow Refraction Seismics*. Chapman Hall, London, 270 pp.
- Trifunac, M.D., 1971. Surface motion of a semi-cylindrical alluvial valley for incident plane SH waves. *Bull. Seismol. Soc. Am.*, 61(6): 1755-1770.